Noname manuscript No.
(will be inserted by the editor)

Behavior of Raman D band for pyrocarbons with crystallite size in the 2-5 nm range

Philippe Mallet-Ladeira · Pascal Puech · Patrick Weisbecker · Gerard L. Vignoles · Marc Monthioux

October 7, 2014

Abstract The pyrocarbon materials investigated here are examples of disordered graphene-based carbons whose crystallite size L_a ranges from 2 to 5 nm. This L_a size range is between two different Raman behaviors, one for which the D band broadens (for $L_a < 2$ nm) and the other for which the D band sharpens (for $L_a > 5$ nm) respectively, with increasing L_a. To fully understand the nature of the G band signal, we checked its wavelength behavior from UV to near IR. We demonstrated that the Raman spectrum is well fitted with simply two Lorentzians with various respective contributions centered at the wavenumber of the D band and a Breit-Wigner-Fano shape for the G band. Each intensity contribution for the D band varies linearly with L_a between 2 and 5 nm while the total D band intensity is nearly constant for excitation wavelengths ranging from 0.532 to 0.638 μm. On the contrary, the integrated intensity ratio D/G follows the well-known L_a^{-1} law. The two sub-bands building the D band are related to the lifetime of the electrons involved in double resonance process which can be scattered twice. Their respective occurrences therefore depend on the crystallite size L_a, when below $\approx$ 5 nm.

PACS 61.72.-y · 76.70.Dx · 78.30.-j · 81.05.U-

1 Introduction

Graphene-based materials are very attractive for many applications. Their very interesting electronic properties are deeply impacted by the presence of point de-

Philippe Mallet-Ladeira, Pascal Puech and Marc Monthioux
CEMES-CNRS, UPR8011,Université de Toulouse, 29 rue Jeanne Marvig, BP 94347, Toulouse, Cedex 4, France E-mail: pascal.puech@cemes.fr

Patrick Weisbecker
CNRS, Laboratoire des Composites ThermoStructuraux, UMR 5801, 3 Allée de la Boëtie, F33600 Pessac, France

Gerard L. Vignoles
Université Bordeaux 1, Laboratoire des Composites ThermoStructuraux, UMR 5801, 3 Allée de la Boëtie, F33600 Pessac, France

fects [1] and edges [2]. As a consequence, the latter have been largely investigated. Raman spectroscopy has become one of the prominent tools for this defect analysis. For graphene-based materials, the spectrum is dominated by two bands. The first one, allowed by Raman selection rules, is called G band. The second one, called D band, is activated by defects and is due to a double resonance process [3]. The recent experimental observation and related modeling reported in Lucchese *et al* [4] prove that two domains should be considered around a defect. The extension of the lattice region electronically impacted by the presence of a defect is about 2 nm. This new vision could explain why the intermediate scale with L_a crystallite sizes around 2 nm in bulk material is so scattered [5,6]. These recent findings open a possibility for a reappraisal of the understanding and treatment of Raman spectra. Tuinstra and Koenig have observed long ago that, for carbon materials whose L_a sizes are above 3-4 nm, the ratio of the D band intensity over the G band intensity extracted from Raman spectra at 0.488 μm is related to the crystallite size L_a determined by X-Ray through $L_a = 4.4/(I_D/I_G)$ [5]. Integrated intensities have been sometimes used [7]. The analysis of large families of disordered carbon materials has been proposed by Ferrari and Robertson [8] in 2002 with two behaviors, one for $L_a < 2$ nm with I_D/I_G varying as L_a^2 based on theoretical considerations and one corresponding to the Tuinstra and Koenig law in L_a^{-1} for L_a higher than 2 nm. The full analysis of the case of $L_a \approx 2$ nm has been addressed experimentally by many approaches leading to empirical laws, but the physical explanation of the change in the relation between L_a and I_D/I_G in the transition domain (2 nm $< L_a <$ 5 nm) is still missing.

Besides, fitting the bands in a Raman spectrum has always been a difficult task. Every Raman specialist around the world has developed his own procedure. Usually, several sub-bands are added until the spectrum is well described [9–11] without any physical consideration. The major problem with this strategy is that the signal explained by the regular vibrational theory and the one coming from a double resonance effect (which is wavelength-dependent through both its intensity and energy) cannot be discriminated. To account for the variations in the background intensity around the G band and in the G band as well, a Breit-Wigner-Fano (BWF) shape has been proposed [12,8]. Indeed, structural disorder activates the phonon density of states as well, which cannot be described by a Lorentzian [8] but tends to a BWF line.

By varying the excitation wavelength from IR to UV, we were able to propose a strategy involving few adjustable parameters to fit the Raman spectra of poorly organised graphene-based carbons, as the only way to treat the Raman spectra with respect to physics. Then, we analyzed the Raman spectra of pyrocarbons using the lowest number of free parameters. The pyrocarbon materials used were quite suitable as model materials for the study as they are exhibiting L_a crystallite sizes right in the range of the above-mentioned transition domain. Thus, we discussed the two broadening values found for the D band and finally observed that the ratio of integrated intensities is better related to L_a^{-1} than the ratio of intensities.

2 Raman experiments

Three kinds of pyrocarbons were selected, and their L_a (L_{a10}) were determined by neutron diffraction. The dimension La_{10} was extracted from the structure factor $S(Q)$ obtained by neutron diffraction [13]. The 10 band and the 004 peak were fitted with split pseudo Voigt functions using the Topas software. Peaks full width at half maximum (FWHM) were corrected for the instrumental broadening using a Ni standard also used for the wavelength determination. Thus, L_a was determined from the corrected FWHM using the Warren formula [14]. The first two pyrocarbons were obtained in an industrial oven [13]: Rough Laminar (RL, L_a = 4.5 nm), and Smooth Laminar (SL, L_a = 3.8 nm). The last one, obtained in a lab-scale reactor, is a Regenerative Laminar (ReL) [15], with a low L_a (L_a = 2.8 nm), though it is as optically anisotropic as the RL.

Raman measurements were carried out without any surface preparation in backscattering configuration at room temperature ($Z(X, X+Y)\overline{Z}$ Porto configuration, X in the layer plane). The laser power was kept low, ($\approx$ 1 mW) in order to prevent heating. Several spectrometers were used: a Dilor UV spectrometer for wavelengths ranging from 0.275 μm to 0.364 μm (4.5 eV to 3.4 eV), a Dilor XY spectrometer with a Ar^+ laser, a T64000 Jobin-Yvon Horiba with a Kr^+ laser, and a XPlora Jobin-Yvon Horiba spectrometer for the 0.532, 0.638 and 0.784 μm wavelengths (2.34, 1.96 and 1.54 eV respectively).

3 Wavelength measurements

In Fig. 1 are reported the Raman spectra obtained for the SL pyrocarbon (crystallite size of 3.8 nm). Both the D and G bands have been fitted by one Lorentzian each, and even if the fit is not good (we will see in the next section how to improve this), a lot of information can be learnt. The data extracted from the fit are reported in Fig. 2. The intensity of the D band lowers and its wavenumber is increased with the excitation energy. In Fig. 2.a, the value of 57 cm^{-1}/eV obtained for the slope of the wavenumber versus excitation energy is close to theoretical predictions [3]. In Fig. 2.a is also reported the G band position. It actually fluctuates but it is clear that there is no significant shift or trend within the whole excitation energy range from infrared to UV. If D' would vary independently of G, the Half Width at Half Maximum (HWHM) as well as the position of the average G band should strongly vary: this is definitively not the case. The D' band is due to an intravalley double resonance process and varies in the same way in intensity as the D band. In the present case, it appears that the D' band has merged with the G band and should not be considered anymore. This is probably due to the small phonon wavevector associated to D' in the double resonance process which is not relevant with small carbon domains. The HWHM of the D band is rather scattered, as a possible consequence of the poor fitting procedure. The apparent HWHM of the D band is nearly twice that of the G band. Finally, in Figure 2.c, the dependence [7] in E^{-4} of the I_D/I_G ratio on the excitation energy is not observed. By normalizing all the spectra with respect to the CaF_2 signal corrected from its wavelength dependence [16], we have observed a maximum of the G band intensity with the green excitation wavelength, in contrast with the case of so-called nanographite [17].

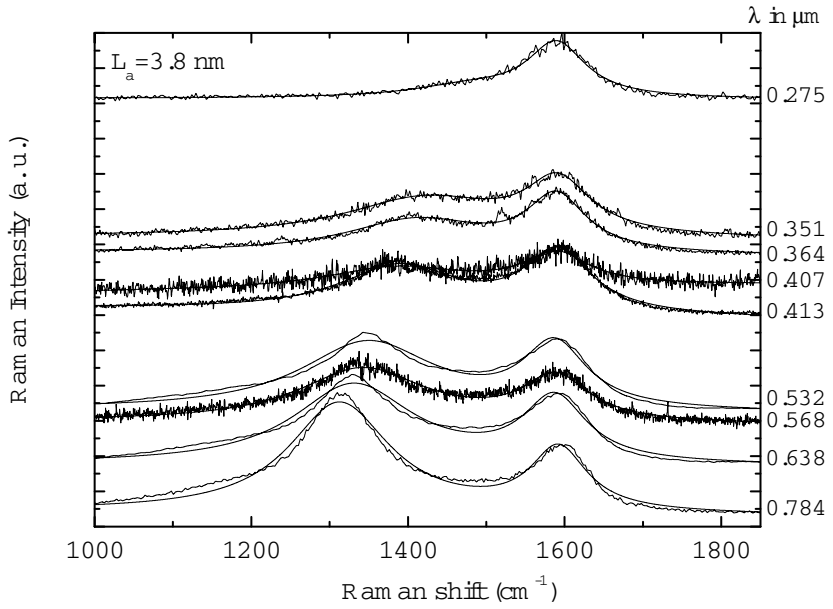

Fig. 1 Raman spectra of SL pyrocarbon (L_a = 3.8 nm) from UV to near infrared. The spacing between the spectra is proportional to the excitation energy. The fitting lines using one Lorentzian for each band and a linear background are also reported. The spectra have been normalized to the G band intensity.

Table 1 Energy (E), wavelength (λ), crystallite size for the broad D sub-band (L_{a2}), crystallite size for sharp D sub-band (L_{a1}), ratio of the D over G band intensities considering the broad D sub-band (I_{D2}/I_G) and sharp D sub-band (I_{D1}/I_G) (see Fig. 3). The last column corresponds to the value of $A_D/A_G \times L_a$.

E(eV)	$\lambda(\mu m)$	L_{a2}(nm)	L_{a1}(nm)	I_{D2}/I_G	I_{D1}/I_G	$A_D/A_G \times L_a$
2.33	0.532	2.3±0.2	4.9±0.2	1.30±0.05	1.12±0.05	9.0±0.5
1.94	0.638	2.5±0.2	4.9±0.2	1.47±0.05	1.34±0.05	10.7±0.5

4 Fitting procedure

The density of vibrational states gives rise to an asymmetric band. Several authors [12,8] have proposed to use a BWF shape for the G band which describes well the spectra of disordered carbons. We used the same approach. The background is described here by a constant. From Fig. 1, any sub-band used to describe the D band should shift at the same rate with the excitation energy. With two Lorentzian bands flanking the D band (not shown) giving three bands, the fit is good but there is no related physical meaning and the number of free parameters is too high to obtain constancy at various wavelengths and with various samples. If we reduce the number of sub-bands down to two Lorentzians, the two bands are now centered at nearly the same position which corresponds to the D band position. One Lorenztian is broad and the other one is sharp. We have observed with all the fitted spectra that the sharp band has a HWHM very close to the value of

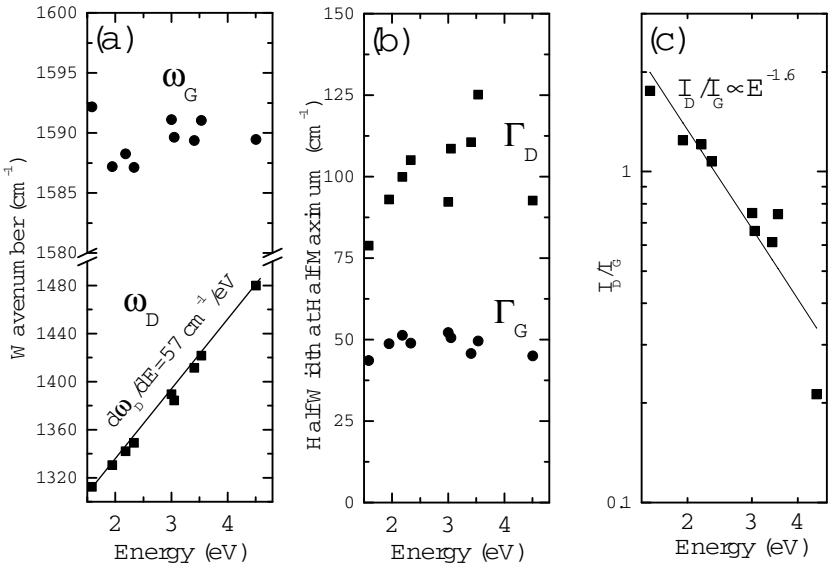

Fig. 2 Wavenumber (a) and HWHM (b) of the G and D bands deduced from the fits reported in Fig. 1 for the SL pyrocarbon. The slope for the D band wavenumber versus the energy excitation is also indicated. (c) I_D over I_G ratio versus the excitation energy in logarithmic scale and a power law fit (line).

the HWHM of the G band. In order to converge quickly, we can use only one parameter for these two quantities or keep them free. We used both strategies and found similar results with spectra obtained using 0.532 or 0.638 μm. Finally, the spectra are fitted by using the following expression:

$$I(\omega) = I_0 + I_{D1}\frac{\Gamma_{D1}^2}{(\omega-\omega_D)^2+\Gamma_{D1}^2} + I_{D2}\frac{\Gamma_{D2}^2}{(\omega-\omega_D)^2+\Gamma_{D2}^2} + I_G\frac{\left(1+\frac{\omega-\omega_G}{q\Gamma_G}\right)^2}{1+\left(\frac{\omega-\omega_G}{\Gamma_G}\right)^2} \quad (1)$$

which contains 10 free parameters corresponding to a constant background (I_0), a double Lorentzian (I_{D1}, I_{D2}, Γ_{D1}, Γ_{D2}) for the D band (same wavenumber ω_D) and a BWF line for the G band (I_G, ω_G, Γ_G, q).

5 Results and discussion

In Fig. 3 are reported the Raman spectra for the three pyrocarbons studied here. The apparent ratio I_D/I_G is nearly constant and could not be explained by a Tuinstra and Koenig law. The fitting with one Lorentzian only for the D band is poor, as demonstrated by the visual difference with Fig. 1 whereas the fitting with a double Lorentzian is nearly perfect (Fig.3). Hence, it is clear that the D band is due to two contributions: a sharp one ($\Gamma_{D1} = 42 \pm 4$ cm^{-1}) and a broad one ($\Gamma_{D2} = 180 \pm 20$ cm^{-1}). In Fig. 4.a is reported the intensity-based I_D/I_G versus

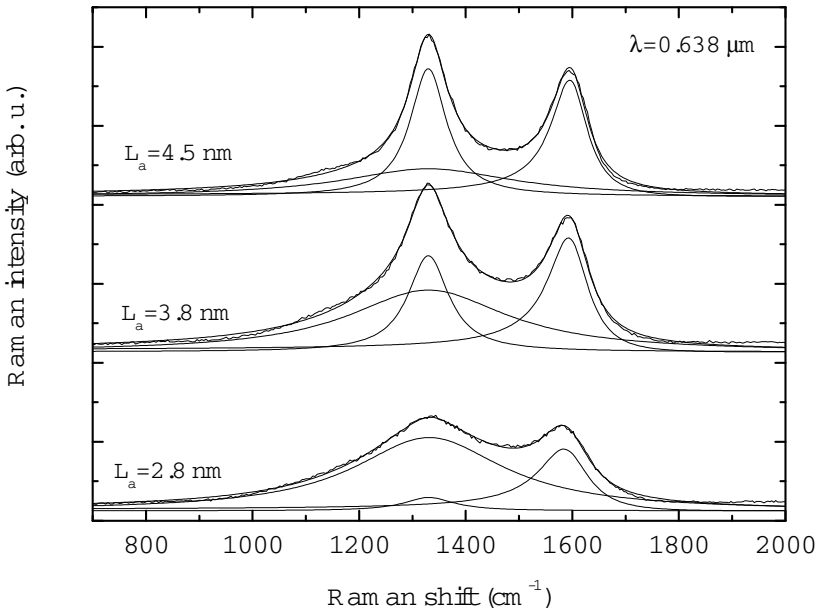

Fig. 3 Raman spectra at room temperature with λ=0.638 μm, along with the fitting curves and the decomposition in 3 bands (two Lorentzians for the D band and a BWF for the G band) according to eq. 1. The fitting is nearly perfect.

the crystallite size and a linear behavior is observed. Two characteristic values are obtained for L_a: the value L_{a1} where the sharp D band is visible and the value L_{a2} where only a broad D band is observed. The crystallite size can then be estimated considering the extreme values I_{D1}/I_G for $L_a = L_{a1}$ and I_{D2}/I_G for $L_a = L_{a2}$.

We have also considered the green excitation wavelength at 0.532 μm. The values are reported in Table 1. Going from green to red, the D band intensity increases as expected. However, the variation of the intensity ratio in E^{-4} proposed by Cançado *et al* [7] is still not observed. In Fig. 4.b are reported the integrated intensities versus the crystallite size. The law in L_a^{-1} is also indicated. For the BWF line corresponding to the coupling of an excitation with a continuum, the G band area is supposed to be proportional to the product of intensity by broadening.

$$\frac{A_D}{A_G} = \frac{I_{D1} \times \Gamma_{D1} + I_{D2} \times \Gamma_{D2}}{I_G \times \Gamma_G} \tag{2}$$

While the product $I_D/I_G \times L_a$ is not constant, the product $A_D/A_G \times L_a$ is nearly constant. The law (see Table 1) is:

$$L_a = \frac{10.7 \pm 0.5}{\frac{A_D}{A_G}} \quad \text{with} \quad \lambda = \ 0.632\ \mu m \tag{3}$$

The Tuinstra and Koenig law (E = 2.54 eV) [5] could be modified to deal with integrated intensities : $L_a \leq 8.8\ (A_D/A_G)^{-1}$ as $\Gamma_D \leq 2 \times \Gamma_G$ with two Lorentzians. With E = 2.54 eV, the value of 8.8 is replaced in Cançado *et al* [7] by 13.5, nearly

the double of the previous value. If we correct this value using the Scherrer factor (K=0.9, 3D ordering) instead of the Warren factor [14] (K=1.84, turbostratic stacking) misused in the cited paper [7] to obtain the crystallite size, all the data become consistent. The probability of the whole process is thus represented by the integrated intensity as expected.

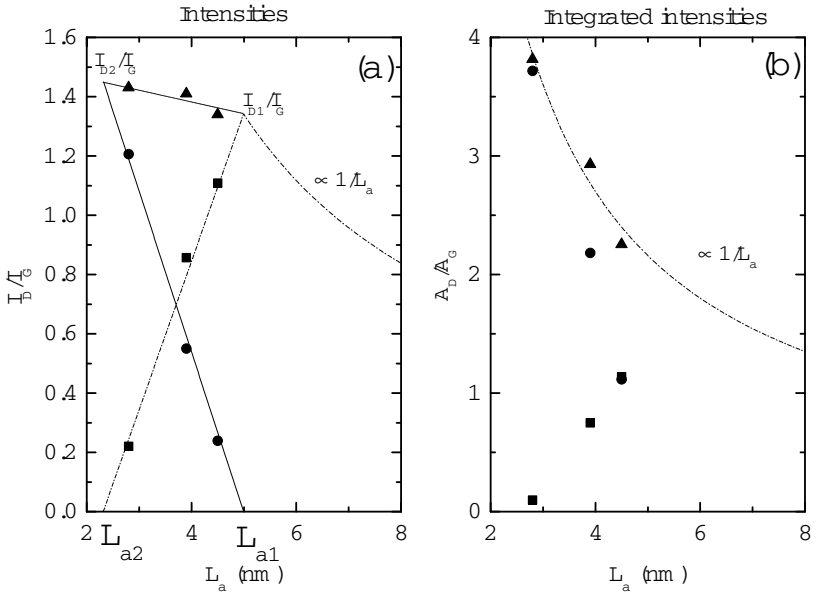

Fig. 4 (a) I_D over I_G ratio from Fig. 3. The decomposition of the D band in (1) a sub-band labelled 1 with a HWHM value very close to that of the G band value with a related crystallite size limit L_{a1} (squares) and (2) in a sub-band labelled 2 with a large HWHM and a related crystallite size limit L_{a2} (dots). The sums of both contributions are represented by triangles. The I_D/I_G regime for $L_a > 5$ nm is also indicated. (b) same as in (a) but with the integrated intensity A.

In Lucchese *et al*'s paper [4], the modeling of I_D/I_G for irradiated graphene is characterized by two quantities corresponding to the structurally disordered region ($r_s = 1$ nm) and the surrounding ordered region characterized by the relaxation length $l = 2$ nm close to theoretical estimates [18]. Recent experimental findings [19] show that the coherence length of the photoexcited electron for the D band in graphene is equal to 3 nm at room temperature. Casiraghi *et al* [20] have estimated the length scale using the uncertainty principle to be 4 nm. In pyrocarbons, each crystallite is bridged to its neighbors by a defect line, few (typically 1-3) carbon-atom thick, *i.e.*, in the range of 0.5 nm or below. This is supported by the high resolution TEM images obtained for long on this well-studied category of materials (for instance [21]). Consequently, L_{a1} and L_{a2} are not related to the extension of the disordered region. If two edges of a same crystallite are closer to each other than $L_{a1} = 4.9$ nm, the electron in the double resonance process is scattered twice. This length of 4.9 nm is close to the length scale obtained with graphene.

Theoretically, Barros *et al* [22] have analyzed multiple scattering effects which reduce the D band intensity for size lower than 16 nm but the HWHM is not discussed. We have applied the same treatment to spectra of multiwall carbon nanotubes (Graphistrength C100 from Arkema company). We found a HWHM of 32 cm^{-1} for D_1 sub-band while the same jump is observed to the HWHM of the D_2 sub-band which is close to 180 cm^{-1}. Therefore, our decomposition should be valid with many carboneous materials. It is worth noting that these HWHM are not sensitive to the excitation energy. It is very likely that the jump in the HWHM value in due to the number of scatterings. The linear behavior observed here is a direct consequence of the scattering length. As the D_1 and D_2 sub-band wavenumbers shift with the exciting energy at the same rate, it is difficult to consider that another phonon branch is at the origin of D_2. With our interpretation, single scattering events correspond to the HWHM of 42 cm^{-1} while double scatterings correspond to 180 cm^{-1}. By increasing the size of the crystallite, the D band originating from one electron scattered twice (D_2) is decreasing until the distance becomes long enough to have only a single scattering signal ($L_a > L_{a1} = 4.9 \pm 0.2$ nm). The associated lifetime was about 5 fs using a Fermi velocity of 1×10^6 $m.s^{-1}$. Calculations including multiple scatterings and interferences would certainly definitively validate this interpretation.

6 Conclusion

In conclusion, the wavelength dependence of the Raman spectra of graphene-based carbon materials with L_a values below 5 nm shows that the width of the G band is constant and that all the components of the D band are due to double resonance processes as their intensities and positions are affected by the excitation energy. The D band has to be decomposed in two contributions centered at the same wavenumber, whose respective occurrences depend on the average crystallite size L_a. This approach reduces the number of free parameters and gives a new insight. The width of the D sub-bands is interpreted as dependent on the number of scatterings as the value jumps from 42 cm^{-1} (single scattering) to 180 cm^{-1} (double scattering). We found a characteristic length of 4.9 ± 0.2 nm which is tentatively associated to the mean free path of the excited electron in our material, beyond which only single scattering events can occur. The integrated intensities of the D over G band ratio allows finding the crystallite size accurately.

Acknowledgements This work was supported by the ANR-funded project ANR-2010-BLAN-929 PyroMaN and the Aerospace Valley network. M. Lalanne, G. Chollon and A. Delcamp (SNECMA) are acknowledged for the sample preparation.

References

1. L.G. Cançado, A. Jorio, E.H. Martins Ferreira, F. Stavale, C.A. Achete, R.B. Capaz, M.V.O. Moutinho, A. Lombardo, T.S. Kulmala, and A.C. Ferrari, Nano Lett. 11, 3190 (2011)
2. C. Casiraghi, A. Hartschuh, H. Qian, S. Pisanec, C. Georgi, A. Fasoli, K. Novoselov, D. Basko, A. C. Ferrari, Nano Lett. 9, 1433 (2009)
3. J. Maultzsch, S. Reich, and C. Thomsen, Phys. Rev. B. 70, 155403 (2004)

4. M.M. Lucchese, F. Stavale, E.H. Martins Ferreira, C. Vilani, M.V.O. Moutinho, R.B. Capaz, C.A. Achete and A. Jorio, Carbon 48, 1592 (2010)
5. F. Tuinstra and J.L. Koenig, J. Chem. Phys. 53, 1126 (1970)
6. D.S. Knight and W.B. White, J. Mater. Res. 4, 385 (1989)
7. L.G. Cançado, K. Takai, T. Enoki, M. Endo, Y.A. Kim, H. Mizusaki, A. Jorio, L.N. Coelho, R. Magalhães-Paniago, and M.A. Pimenta, Appl. Phys. Lett. 88, 163106 (2006)
8. A.C. Ferrari and J. Robertson, Phys. Rev. B. 61, 14095 (2000)
9. M.R. Ammar and J.N. Rouzaud, J. Raman Spec. 43, 207 (2012)
10. T. Jawhari, A. Roid, and J. Casado, Carbon 33, 1561 (1995)
11. A. Sadezky, H. Muckenhuker, H. Grothe, R. Niessner, and U. Pöschl, Carbon 43, 1731 (2005)
12. D.G. McCulloch, S. Prawer, and A. Hoffman, Phys. Rev. B. 50, 5905 (1994)
13. P. Weisbecker, J.M. Leyssale, H.E. Fischer, V. Honkimäki, M. Lalanne, G.L. Vignoles. Carbon 50, 1563 (2012)
14. B.E. Warren BE, Phys. Rev 59, 693 (1941)
15. X. Bourrat, A. Fillion, R. Naslain, G. Chollon and M. Brendle, Carbon 40, 2931 (2002)
16. M. Grimsditch, M. Cardona, J.M. Calleja and F. Meseguer, J. Raman Spec. 10, 77 (1981)
17. L.G. Cançado, A. Jorio, and M.A. Pimenta, Phys. Rev. B 76, 064304 (2007)
18. D.M. Basko, Phys. Rev. B 79, 205428 (2009)
19. R. Beams, L.G. Cançado, and L. Novotny, Nano Lett. 11, 1177 (2011)
20. C. Casiraghi, A. Hartschuh, H. Qian, S. Pisanec, C. Georgi, A. Fasoli, K. Novoselov, D. Basko, and A. C. Ferrari, Nano Lett. 9, 1433 (2009)
21. A. Oberlin, Carbon 40, 7 (2002) 7
22. E. B. Barros, K. Sato, Ge. G. Samsonidze, A. G. Souza Filho, M. S. Dresselhaus, and R. Saito, Phys. Rev. B 83, 245435 (2011)